FREQUENCY MODULATION

TO INCREASE RADAR WEATHER INFORMATION

by

Bernard Antony Stevens B.Sc.

A Thesis Submitted to the Faculty of Graduate Studies and Research of McGill University in Partial Fulfilment of the Requirements for the Degree of Master of Science.

Montreal, P.Q. August 1952.

ACKNOWLEDGEMENTS

The work reported in this thesis was carried out under the direction of Professor J. S. Marshall. The author is endebted to Dr. Marshall for his criticism and advice, and also to other members of the Stormy Weather Research Group of McGill University, notably Mr. T. W. R. East, who was responsible for the design of an electronic circuit used in the work.

Acknowledgement is also due to the Defence Research Board for financial assistance received through a grant to Dr. Marshall.

FREQUENCY MODULATION
TO INCREASE RADAR WEATHER INFORMATION

Table of Contents

ABSTRACT

Theoretical considerations indicate that frequency modulation of a weather radar allows a more rapid determination of the long term average echo intensity from several instantaneous echoes. The modulation should be sawtooth in waveform, of period 100c/s and amplitude 10Mc/s for an AN/TPS 10 radar. Use of a rotating vane in the waveguide gave a sinusoidal modulation of period 100c/s and amplitude 8 to 10Mc/s. The local oscillator was kept in step with the magnetron by a sawtooth modulation. The use of the microwave gyrator as an improvement on the rotating vane is suggested.

Chapter 1

HOW THE NEED FOR FREQUENCY MODULATION ARISES

Nature of echo from extended target

The use of radar for observing atmospheric precipitation brings to the foreground the problem of the interpretation of the echo received from a set of scatterers randomly distributed along the length of the radar pulse.

Examination of this question leads to the following result (Marshall and Hitschfeld, 1951). At any given time, the echo received and displayed on the radar screen has come from points at distances along the beam within one half pulse-length (figure 1.1). This is because the front edge of the pulse left the radar at a time τ before the back edge. Hence

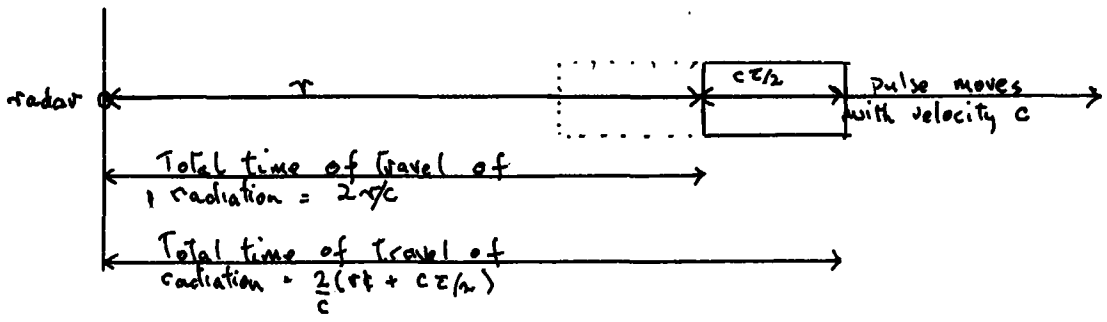

Figure 1.1 Time required for echoes to return to radar.

---

echoes from the front, while taking $\tau/2$ longer to return

to the radar than echoes from the middle of the pulse, started out exactly that much earlier.

If an extended target, such as rain, is being viewed, this half pulse-length contains a number of drops randomly distributed in distance from the radar, and so there is a random distribution of the phase of the echo received from the individual particles. The total echo is the phasor sum of the individual echoes.

Distribution of A^2

This total echo is measured by A^2, the intensity of the signal received. This intensity fluctuates as the drops take on different configurations. The quantity we wish to know is $\overline{A^2}$, the average of very many measurements of A^2. The distribution of the values of A^2 is given by

$$P(A^2)\, dA^2 = \frac{1}{\overline{A^2}} \exp\left(-\frac{A^2}{\overline{A^2}}\right) dA^2$$

and is represented graphically in figure 1.2

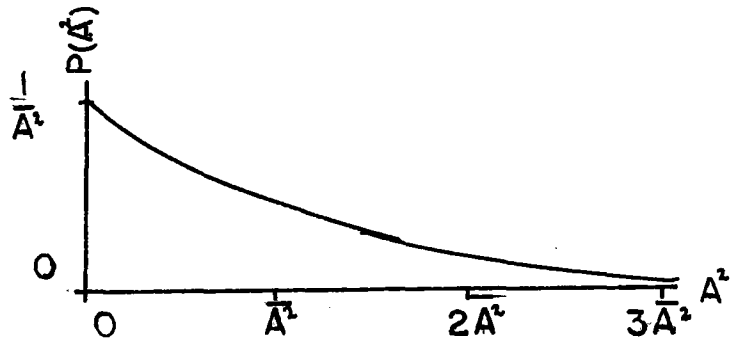

Figure 1.2 Probability distribution of A^2 for a single measurement.

This shows us that the figure we get if we make a single measurement of the echo from a given volume of space, may have any value from zero to a very large value, with a most probable value of zero. So a single measurement does not yield much information.

Improvement with several measurements

If we make k independent measurements on the same volume of space and average the values of A^2, we get a different distribution, depending on the value of k, which gets more peaked as k increases. The most probable value of intensity is $A^2 \cdot (1-\frac{1}{k})$. Figure 1.3 illustrates the case for k=100.

Importance of independent values of A^2

Now the important thing is that successive measurements of A^2 be independent, i.e. that the distribution in phase of the particles change from one measurement to the next. If the distribution does not change, the second measurement can only differ from the first in phase, not in amplitude, and since our receiver is not phase sensitive, the two measurements have only the worth of one.

Figure 1.4 illustrates the point. The drops are here assumed to have equal scattering power.

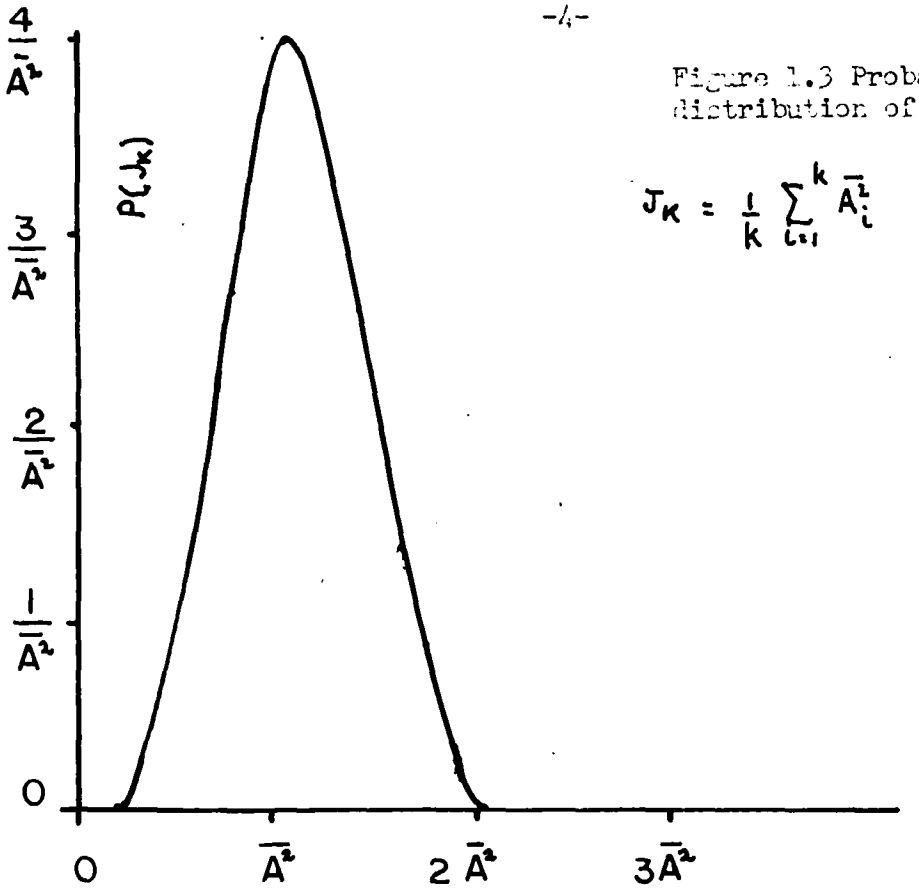

Figure 1.3 Probability distribution of J_{100}

$$J_K = \frac{1}{k} \sum_{i=1}^{k} \bar{A}_i^2$$

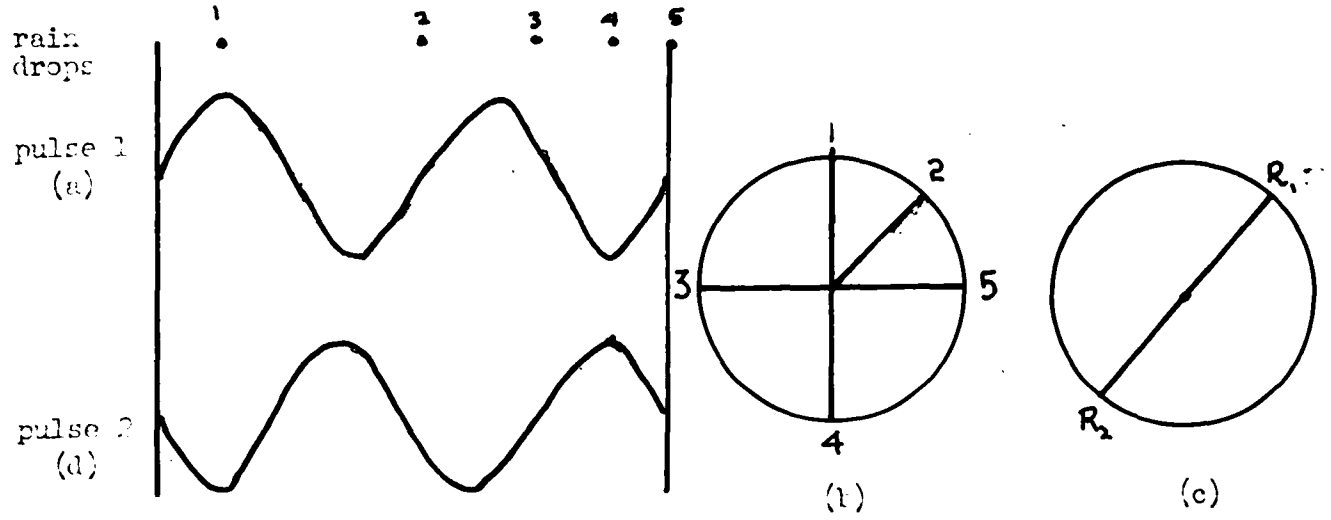

Figure 1.4 Phasor sums of individual echoes (a) represents the first pulse. The contributions from the drops are summed by phasor diagram (b) to give resultant R_1 (c). Now the second pulse (d) is out of phase with (a) by π radians. This means that in (b) we rotate our axes to get the new resultant R_2. Clearly this can only change the phase, not the magnitude of the resultant.

Independence by reshuffling

If the particles shuffle about, and have reached a new distribution when the new pulse comes along, the resulting measurement of A^2 will be independent of the first.

It is believed (Marshall and Hitschfeld, page 26) that rain drops reshuffle sufficiently to give independence in about 0.02 to 0.01 second. In the radar set used, the PRF is 1000*; at least 10 pulses are sent out in this reshuffling time, and so only the first and the last give independent measurements of A^2.

Independence by scanning

Another way in which independence is achieved is by sending the pulse into a different volume of space. The width of the beam in azimuth is 2°, and this is the limiting factor for resolution. The elevation width is ½°. Since we must assume homogeneity of the precipitation over 2° of azimuth, it is reasonable to assume it over 1° of elevation. This permits us to regard the echo from two adjacent beam widths as independent measurements of A^2 with the same $\overline{A^2}$ (figure 1.5).

Our beam, ½° wide, scans 25° in ½ second. Hence it moves 0.1 beam width between pulses, which gives us the same number of independent measurements as the consideration of reshuffligg i.e. 1 per 10 pulses.

---

*For complete specification of the radar used see Appendix 1.

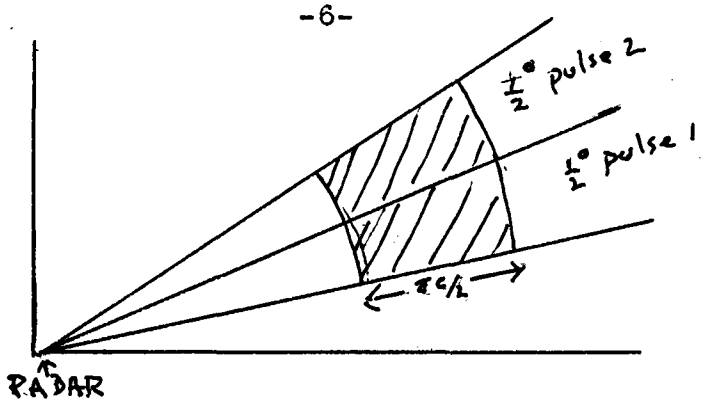

Figure 1.5 Adjacent volumes of space scanned by the radar.

Independence by frequency shift

The intervening measurements, only partly independent, are not completely valueless, but it has been shown (Marshall and Hitschfeld, page 35) that they contribute very little to our knowledge of $\overline{A}^2$. Our problem is to find a way of making the echo from these pulses usable, and to this end we turn to frequency modulation.

To understand the effect of shifting frequency from one pulse to the next consider figure 1.6. Here there is one wavelength more in pulse 1 than in pulse 2. The effect is that of a vernier scale. A given phase is "smeared out" over the whole pulse-length. Consequently the distribution in phase of the drops is as completely altered as if they had reshuffled.

Effective degree of independence

The exact degree of independence achieved for a given frequency shift has been calculated (Marshall and Hitschfeld, page 41). To express it we introduce k_e, the

worth of a given measurement, so that

$$k' = \sum_{i=1}^{k} (k_e)_i$$

is used instead of k as the number of independent measurements.

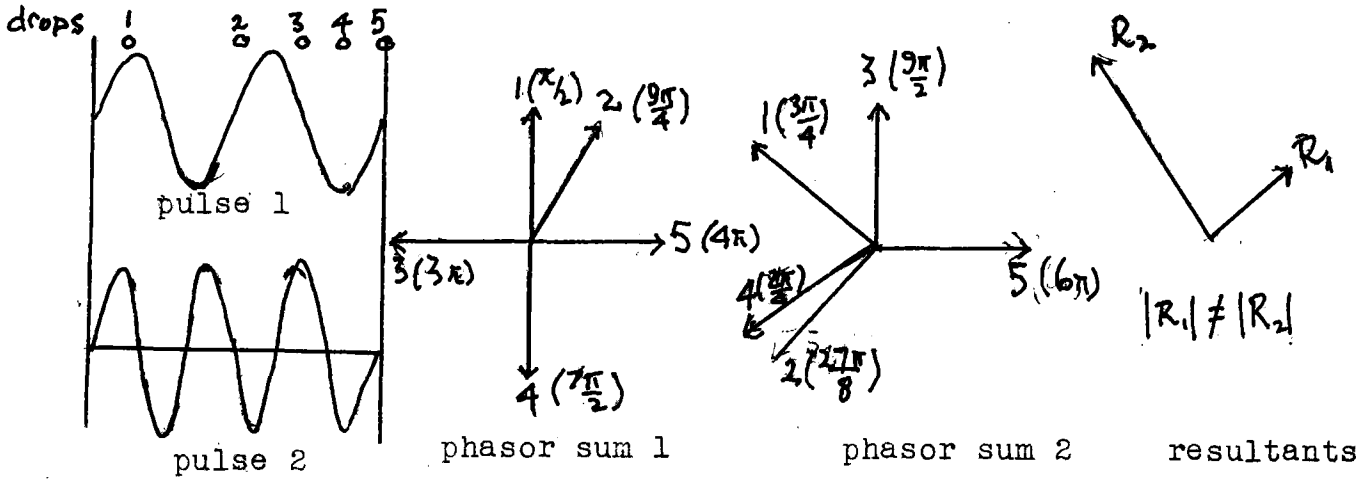

Figure 1.6 Phasor sums of individual echoes (frequency shift).

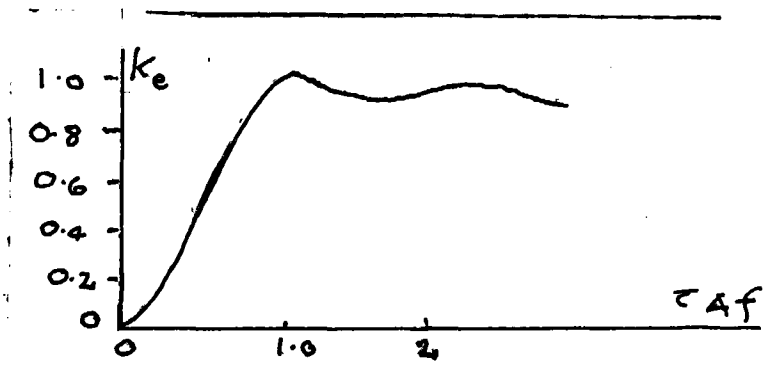

Figure 1.7 k_e the measure of independence of successive echoes, against $\tau\Delta f$

For complete independence $k_e = 1$, for complete dependence $k_e = 0$. For instance, if we have four measurements, the first independent, the second dependent, the third and fourth half independent, we put $k' = 1 + 0 + \frac{1}{2} + \frac{1}{2} = 2$, and say that we have effectively two measurements.

Now $k_e = 1-\left(\frac{\sin \pi \tau \Delta f}{\pi \tau \Delta f}\right)^2$ where τ is the pulse-length, and Δf the frequency shift from one pulse to the next. This function is represented graphically in figure 1.7.

It is seen that independence is achieved for $\tau \Delta f = 1$ and that we can allow values of $\tau \Delta f$ down to about $\frac{2}{3}$ without sacrificing much independence.

Specifications of frequency modulation

This means, for our radar (PRF=1000, $\tau = 10^{-6}$ sec.) a frequency shift of 1M$^c/_s$ from pulse to pulse. As we saw earlier, reshuffling has given independence after about 10 pulses, so we need only shift frequency for this number of pulses, and then "fly back" to our original frequency. The desired modulation envelope is then a sawtooth wave of amplitude 10M$^c/_s$, frequency 100$^c/_s$, as illustrated in figure 1.8.

At the same time, the power output must not alter. A change would have the effect of weighting the different measurements. A change of more than 1 db. cannot be allowed.

Frequency modulation will do for us quickly what natural reshuffling does relatively slowly. We already make use of the latter process by taking time exposures of the radar screen, thus obtaining 1000 independent measurements in 10 seconds. Frequency modulation is

intended to compress these 1000 measurements into 1 second, so as to make a 1 second exposure with frequency modulation as useful as a 10 second without. The effect in terms of photography is to make the picture less grainy, since there is less fluctuation of the value of $\vec{A}_K$ about the mean ($\bar{\vec{A}}$). Figure 1.9 comparing a 1 second exposure with a 10 second, at fixed frequency, illustrates this.

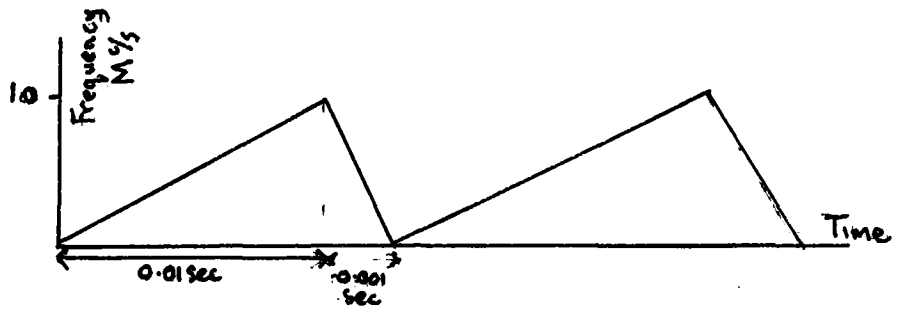

Figure 1.8 Required modulation envelope

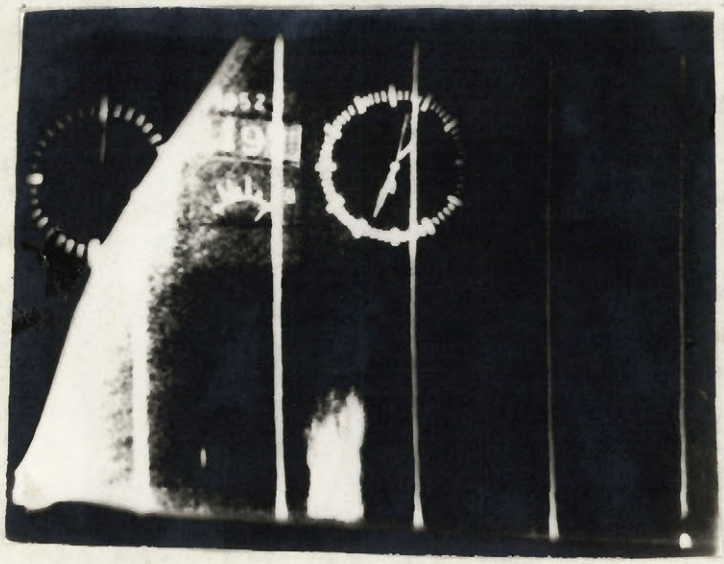

One second exposure

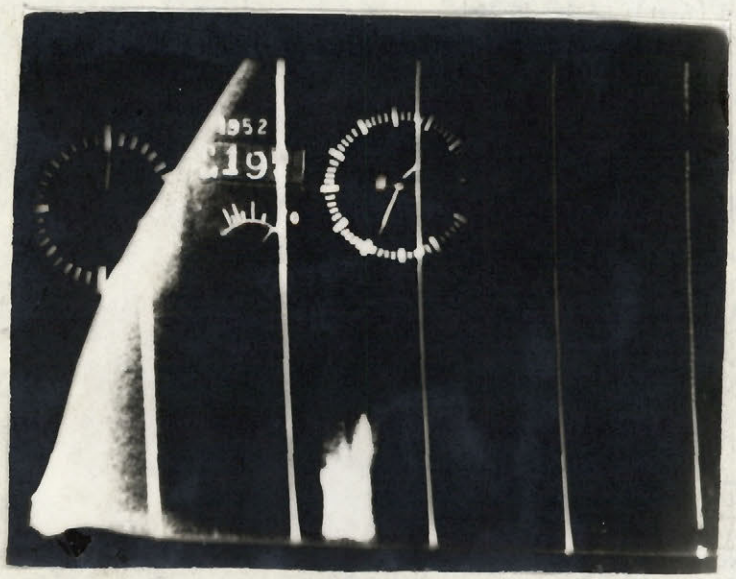

Ten seconds exposure

Figure 1.9 A 1 second and a ten seconds exposure, taken 15 seconds apart at fixed frequency, of the same precipitation.

Chapter II

FREQUENCY CHANGE IN A MAGNETRON

Theory of magnetron operation

The magnetron as it is ordinarily operated is a travelling wave tube. Figure 2.1 represents a waveguide loaded by resonant cavities, the effect of which is to slow down the velocity of an electro-magnetic wave travelling down the guide. Between top and bottom is a D.C. potential, the top surface positive. Electrons leave the lower surface of the waveguide, and travel toward the

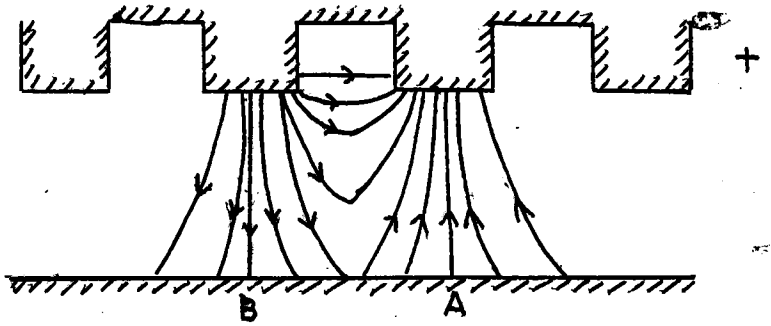

Figure 2.1 Loaded waveguide as a travelling wave amplifier.

---

upper, at the same time moving along the guide at the velocity of the wave. Lines of electric force are shown for the wave. The whole picture may be supposed drawn in coordinates moving with the wave, so that the electron path is straight across the tube. An electron leaving the cathode at A will be decelerated during the whole of its transit by the R.F. field, and so will give up energy to the R.F. field,

obtaining it from the D.C. field. An electron leaving at B will draw energy from the R.F. field.

To make this a successful amplifier of the R.F. wave requires, (1) the electrons move along the tube at the same velocity as the e/m. wave ; (2) the electrons which take energy from the wave be removed. To make a successful oscillator requires in addition, (3) the tube be frequency selective.

These conditions lead us to the magnetron. The electron path in the crossed magnetic and electric fields is similar in cylindrical symmetry to the epicycloid of plane symmetry. To satisfy condition (1) we must arrange that the velocity of the center of the rolling circle keeps the electrons in step with the R.F. field. This can be done by a proper choice of magnetic and electric fields.

Condition (2) is then satisfied automatically; the increase in velocity of electrons aided by the R.F. field increases their rolling circle radius, and takes them out of the interaction space. Electron paths are shown in figure 2.2.

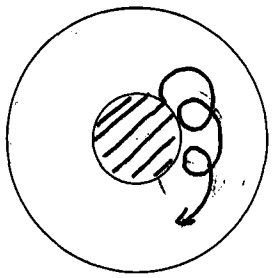

(a) Generation of an epicycloid by a rolling circle.

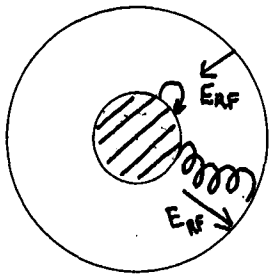

(b) Electron paths in a magnetron.

Figure 2.2

The third condition is satisfied because the distance round the anode must be an integral multiple of a wavelength. This gives us a number of possible frequencies, and a method is available (strapping) of separating one of them sufficiently from the others for satisfactory operation.

Validity of circuit concept

The integral $\oint \mathbf{E} \cdot d\mathbf{l}$ is independent of the path if we do not leave the interaction space. Hence we can by means of it define V_{RF}, the R.F. voltage in the electron stream. The meaning of the electron current is obvious, and the current may be directed at any angle to the field. Hence, current and voltage being properly defined, and all phase relationships between them being possible, we may introduce Y_e, the admittance seen looking from the cavities into the electron stream. This is defined as $\frac{I_{RF}}{V_{RF}}$.

Condition for oscillation

V_{RF} is common to both electron stream and cavities, and the current flowing from cavities into electron stream must be equal and opposite to that flowing from cavities to load. Hence if Y_s is the admittance seen from the cavities looking toward the load, for $V_{RF} \neq 0$,

$$Y_e = -Y_s$$

This is a general condition for oscillation in tubes.

Frequency determining relation

The cavities and load can certainly be represented

by lumped parameter circuits, so from now on we can use that concept in discussing the problem. The appropriate transformations will not be given but only the end result. The above condition reduces to

$$G_e + G_c + k_1 G_L = 0$$
$$B_e + k_2\omega + k_1 B_L = k_3$$

where G_e, B_e, G_c, B_c, G_L, B_L, are the conductance and susceptance of the electron stream, cavities and load, respectively, k_1, k_2, k_3 are constants, and ω the angular frequency of operation.

(References: Slater, Microwave electronics.
R.L. series Volume 6, chapters 6 & 7.)

Methods of varying frequency

To vary the frequency we might first consider keeping B_L fixed and varying B_e. This could be done by varying the magnetic and D.C. electric fields. The result can be obtained from the performance chart of the magnetron, a simplified version of which is seen in figure 2.3

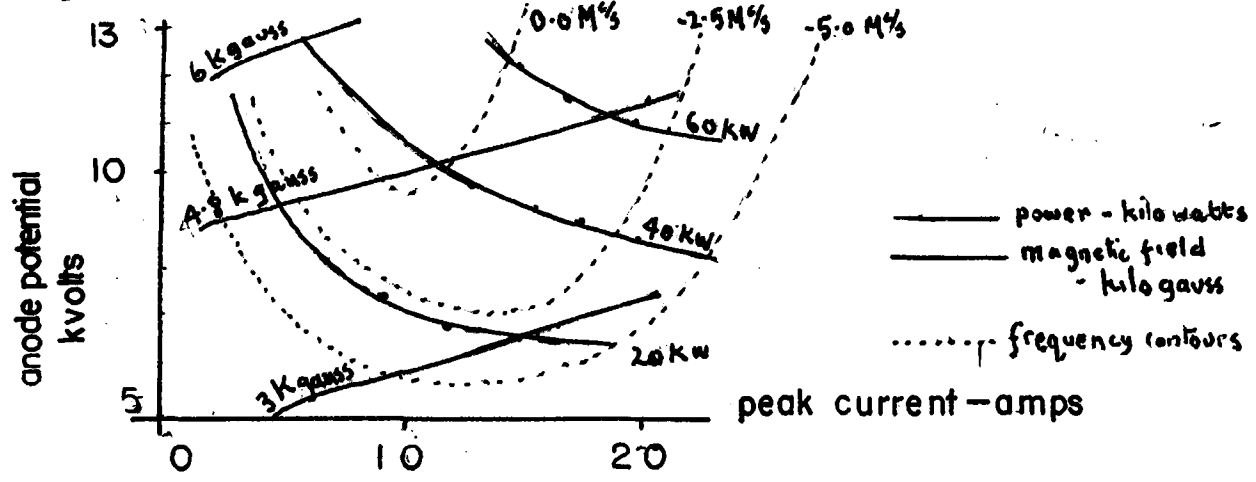

Figure 2.3 Magnetron 2J49 performance at constant load.

In this diagram we see lines of constant power. To follow them means changing the magnetic field and the anode potential simultaneously by large amounts, with accompanying changes in anode current. Even then frequency changes only occur at certain points of the operating region. The difficulties of this method need not be emphasised.

Instead, let us look at the effect of varying B_L.

Changing load impedance

If G_L is kept constant, G_e remains constant, and so the power output ($\propto V_{RF}^2 . G_e$) remains constant. So this seems a suitable method of varying the frequency. The behaviour of a magnetron at constant magnetic field and anode voltage as B_L and G_L vary is seen from the Riecke diagram.

The Riecke diagram is plotted on a Smith chart, i.e. half the G, B, plane transformed into a circle (figure 2.4). To express the variables in terms of quantities easily measured, the standing wave ratio r and its phase θ are introduced as polar coordinates.

Refering to figure 2.5, the circles of constant B_L do not coincide with the lines of constant power as in the idealised case treated above, but by varying G_L and B_L simultaneously we could keep to a constant power contour. At all powers the frequency swings we want are attainable.

So our task is to vary the standing wave ratio in the waveguide in magnitude and phase to an amount which is to be determined from the Riecke diagram.

Electric tuning

A further possible method of varying the frequency is changing the electronic admittance in the cavities. This is achieved by means of a stream of electrons coming from an auxiliary cathode, and modulated by a grid.

This is the most convenient method, since it is purely electronic. Unfortunately it demands a special magnetron, and a suitable one for our radar set is not manufactured at present.

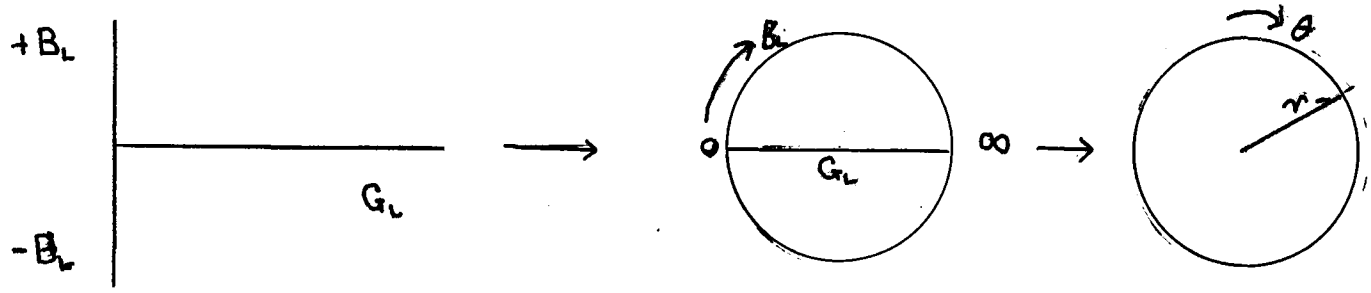

Figure 2.4 Evolution of the Smith chart.

TECHNICAL INFORMATION
MAGNETRON OSCILLATOR

AVERAGE PERFORMANCE CHARACTERISTICS

FREQUENCY-POWER CONTOUR DIAGRAM

Average locations of frequency convergence for the 2J49 and 2J50 are indicated on the circumference of diagram.

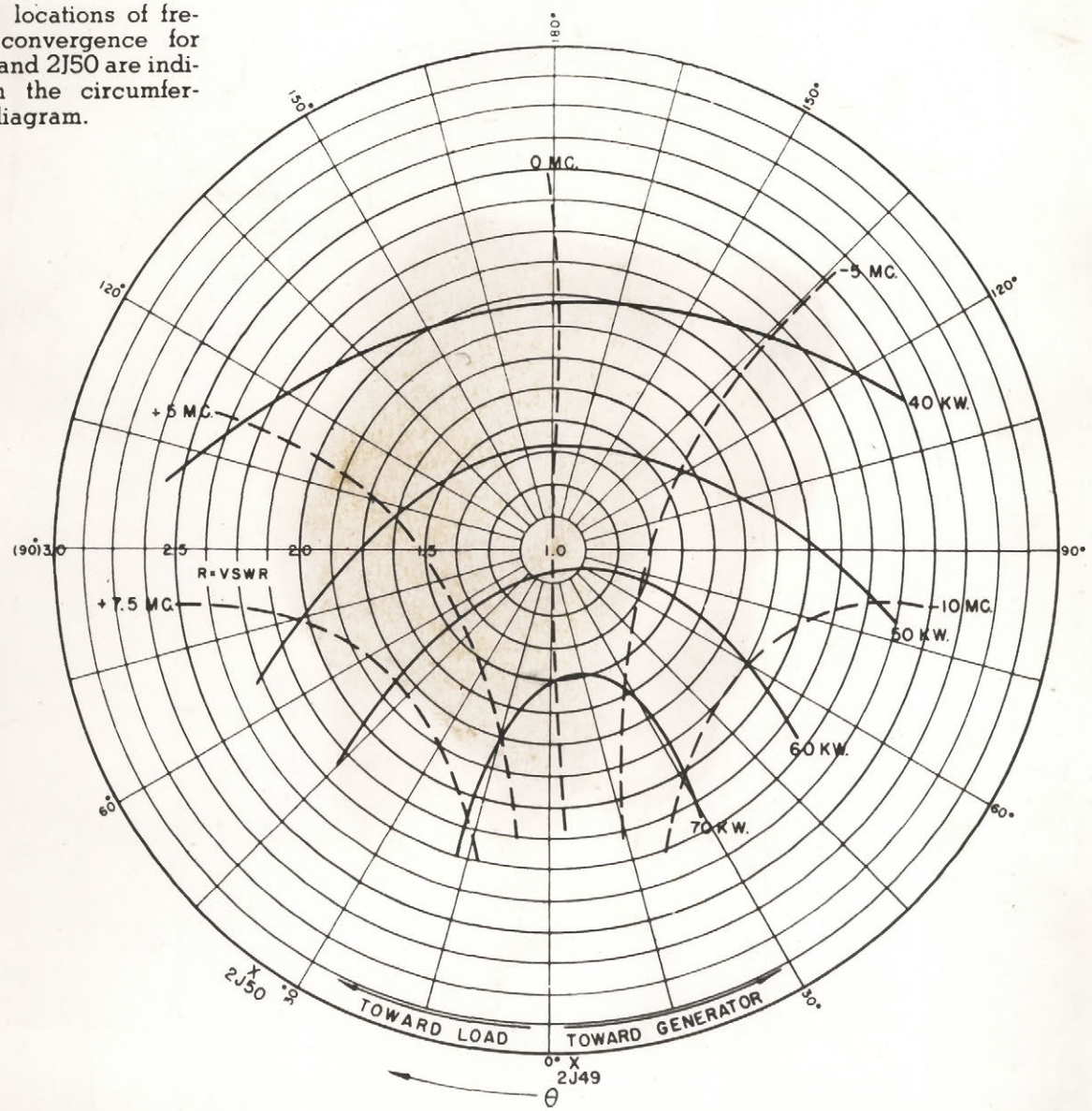

OPERATING CONDITIONS

Recurrence rate = 1000 CPS
Pulse width = 1 microsecond
Magnetic field = 5400 gauss
Peak magnetron current = 12.0 a.
Recommended load for 2J49-2J50 at center of diagram.

RIEKE DIAGRAM

R = Standing wave ratio in voltage.
θ = Distance of standing wave minimum from face of output flange of tube toward load.
—— = Power contours (peak Kw.)
– – = Frequency contours (megacycles deviations from frequency of magnetron feeding into a matched line).

Chapter III

PRACTICAL DETAILS OF THE METHOD USED

Frequency modulation of the radar AN/TPS 10 can be discussed under three headings:

(a) Frequency change in the transmitter.

(b) Tuning of the receiver.

(c) Monitoring the frequency shift.

Frequency change in the transmitter

Application of the theory of chapter II encounters an immediate difficulty - that of constructing the Riecke diagram for the magnetron in actual use. The data supplied by manufacturers are of little use, because the point on the chart at which our magnetron is working before we introduce frequency modulation is not known, i.e. we do not know the magnitude of the standing waves in our waveguide and their phase relative to the output flange of the magnetron, and we do not know the power output of the magnetron.

Since our radar set is in the open air in a rather awkward position, carrying out the measurements necessary to determine these things would not be easy, though not prohibitively difficult. Moreover once they were determined, it would not be an easy task to design an impedance that would give the necessary locus on the Riecke diagram. So it was decided, as a first step, to attempt the frequency

change without making a calculation.

Method used

An obvious way of moving about the Riecke diagram is to introduce a variable reflector into the waveguide. This takes the form of a rectangular plate of dielectric which can be rotated so as to present either its face or its edge to the radiation (figure 3.1). As it is spun round

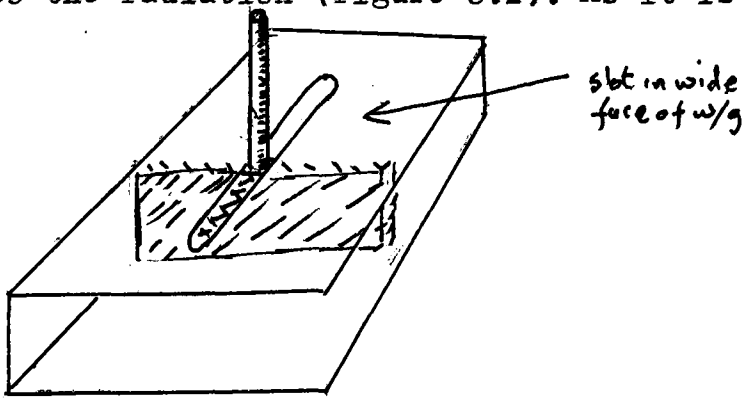

Figure 3.1 Dielectric vane inserted in the waveguide to set up standing waves.

it varies the amount of reflected power cyclically at twice the rotation frequency. Thus we require a rotation at 3,000 rpm to give 100% modulation frequency. Polystyrene was chosen as the dielectric because it combines a reasonably high dielectric constant at microwave frequency with a low loss tangent.

Quality of the waveform

We are satisfying ourselves with a sine wave modulation, or something approaching that, instead of the sawtooth which would be ideal. This means that we do not get independent measurements from the pulses that occur at the turning points

of the wave form, since 0.01 second has not elapsed since the frequency had that value previously (figure 3.2).

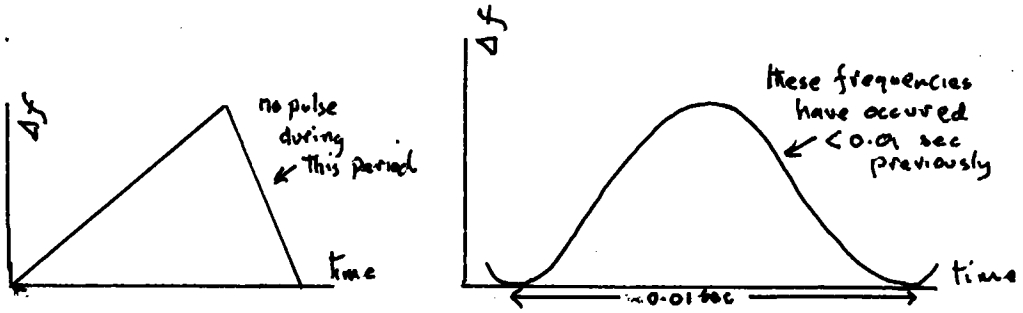

Figure 3.2 Effect of departure from sawtooth waveform.

Thus successive measurements after the peak of the frequency is passed will have k_ℓ rising from near zero to 1.

Effect of bad waveform

An attempt will be made to estimate the degree of independence obtained with the sinusoidal waveform. Figure 3.3 shows the frequencies of the successive pulses. It will be assumed that the degree of independence due to reshuffling is proportional to the time elapsed, and rises to k 1 in 10 pulse lengths.

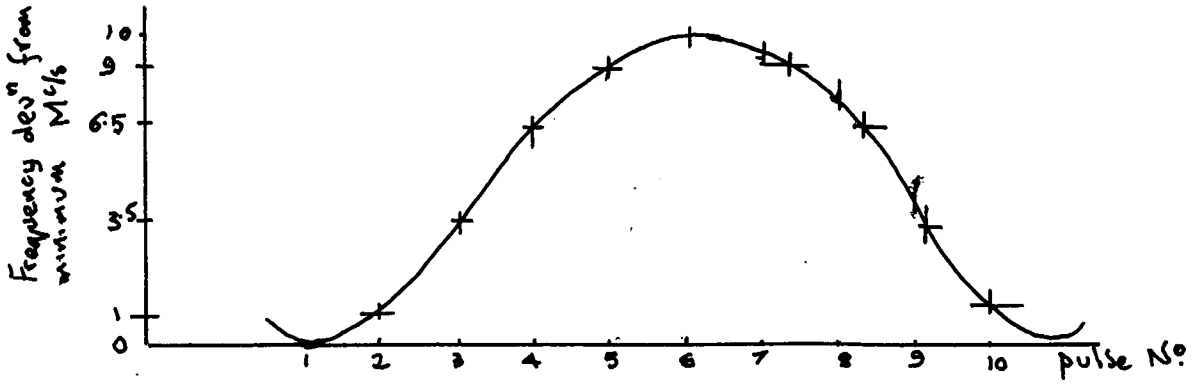

Figure 3.3 Frequencies of successive pulses under a sine envelope.

From the diagram we see that pulses 7,8,9,10, have frequencies equal to those of pulses 5,4,3,2, respectively. Echoes from the former pulses are not independent therefore. Their k_e due to frequency modulation is equal to zero. But the elapsed time from pulse 5 to pulse 7 is 0.002 second, and by our assumption this gives a k_e due to reshuffling of 0.2. Similarly we calculate the k_e due to reshuffling of each of the later pulses.

Finally we assume that the total k_e is the sum of the k_e's due to the two different causes. Making the calculation leads to a total k_e of 8.2.

Thus we lose 18% of our information due to poor waveform.

Test on waveform

An actual test performed with a lucite vane gave the waveform shown in figure 3.4 . This test was performed with the vane at rest, and rotated by hand to the different positions. The frequency was measured with a cavity wavemeter and a crystal detector. The transmitter bandwidth is roughly 2½% (Bandwidth is is considered further at the end of this chapter).

Lack of symmetry in the vane, resulting in one end being nearer the magnetron in the $\pi/2$ position than the other end in the $3\pi/2$ position, makes one peak higher than the other.

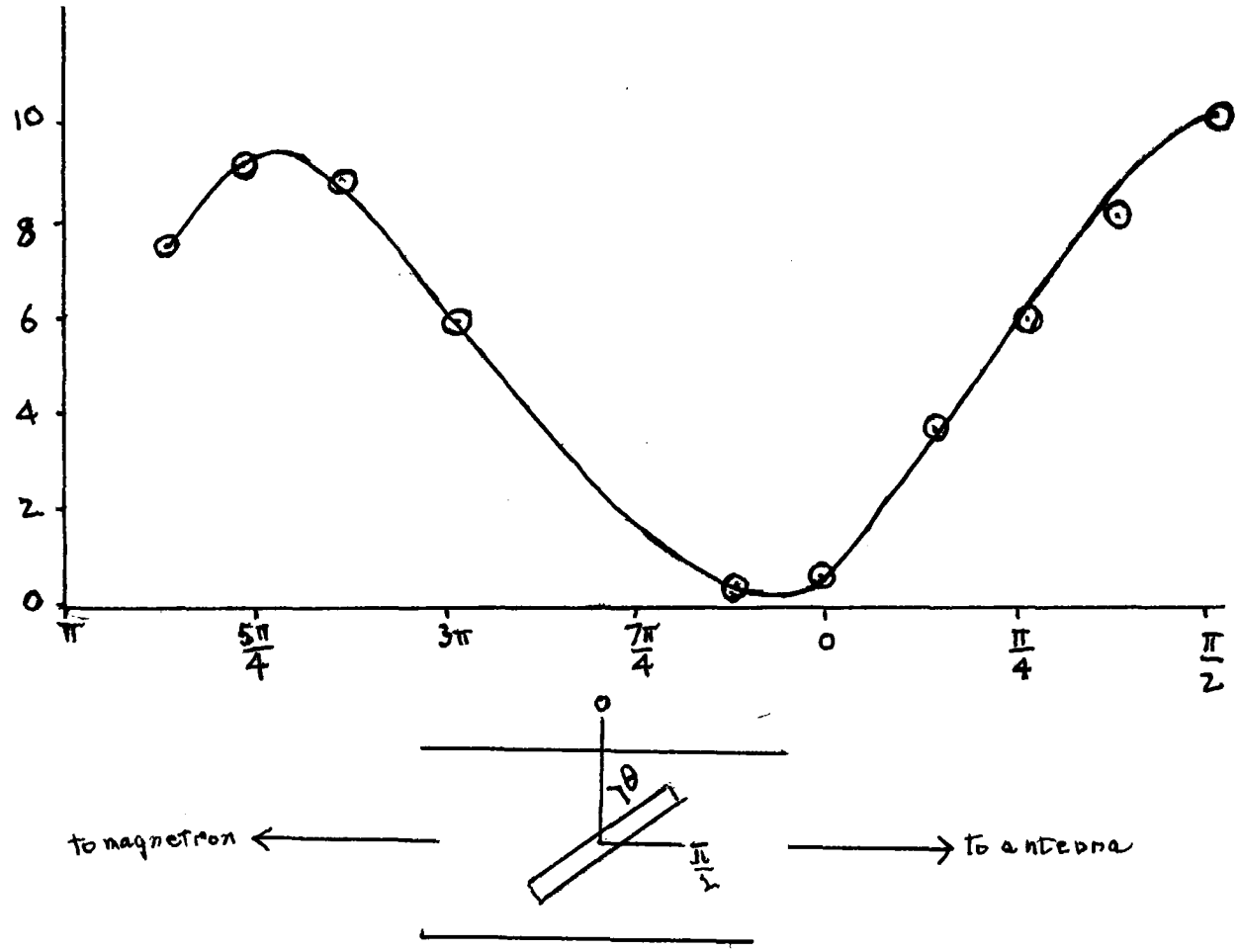

Figure 3.4 Waveform of modulation envelope as obtained by a static test. Lucite vane, $\frac{3}{8} \times \frac{5}{8} \times \frac{1}{8}$ inch.

Tuning the receiver

The bandwidth of the receiver is about 3M$^{c}/_{s}$, and we are changing the transmitter frequency by 10M$^{c}/_{s}$. An A.F.C. circuit is provided in the receiver, but it is designed to cope with pulling as the antenna scans, i.e. pulling at a rate of not more than 300M^{c}/s/second. We are changing the frequency at a rate of 1,000M^{c}/s/second, and the A.F.C. cannot follow as quickly as that.

It seems best for a first trial to dispense with A.F.C. The radar magnetron does not pull in fact, as the antenna scans, so for short periods of time, it can be relied on to stay at constant frequency. The klystron reflector voltage can then be swept at the modulation frequency by a conventional sweep circuit giving the waveform of the modulation envelope, and triggered by a shutter on the revolving shaft of the frequency shifting vane. It is not necessary to follow the waveform of the modulation exactly; the bandwidth of the receiver allows some latitude.

The sweep on the klystron reflector is most easily made linear, not sinusoidal. It would be quite difficult to make a sinusoidal sweep lock in with the magnetron frequency- even the generation of a 100 $^{c}/_{s}$ sine wave requires bulky components.

However as figure 3.5 shows the klystron frequency with a linear sweep never moves farther from the

correct frequency than 1M/s, well within the receiver bandwidth.

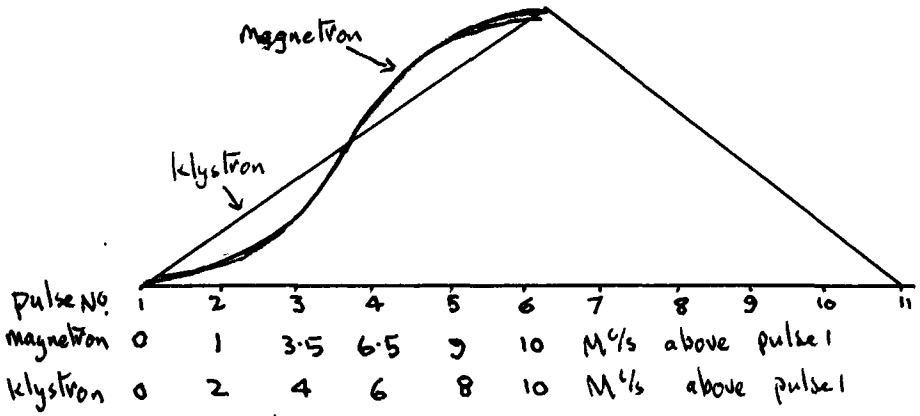

Figure 3.5 Difference in waveform between magnetron frequency sweep and klystron frequency sweep.

The circuit of the klystron sweep generator is shown in figure 3.6*. The light shining on the phototube is interrupted by a shutter on the shaft of the vane twice per revolution. When this happens the grid of tube 1 rises to approximately 300 volts; the cathode potential rises to about 300 volts and tube 2 starts to conduct, running its anode potential down, feed back from anode to grid through C keeping the fall linear. When the light shines on the phototube again the grid of tube 1 goes to about ground potential, the tube is cut off and the voltage of the cathode goes down. Tube 2 is cut off gradually and the potential of the anode runs up.

---

* This circuit was designed by Mr T.W.R.East.

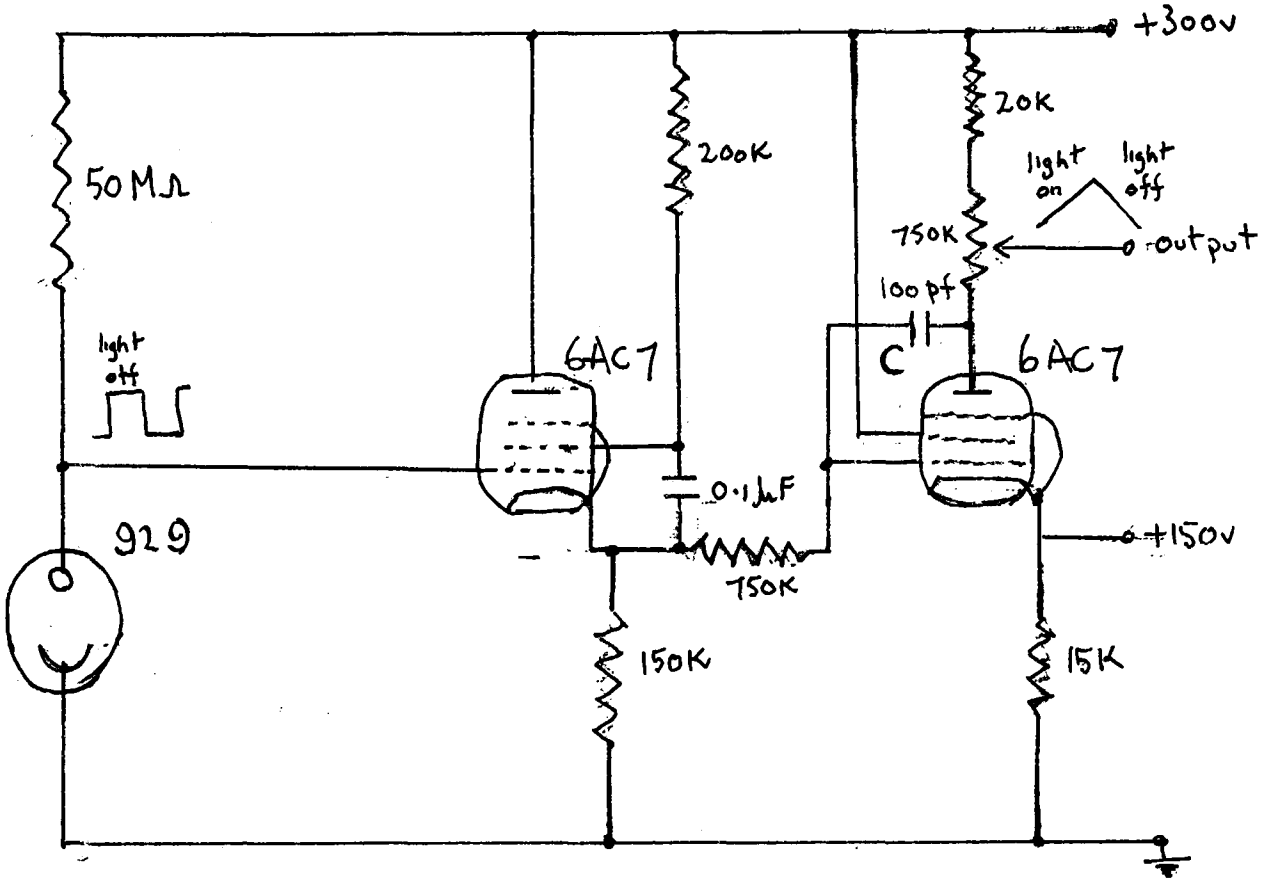

Figure 3.6 Circuit of the klystron sweep generator with waveforms.

Monitoring the frequency shift. Bandwidth and pulse shape

The output of our transmitter consists , ideally, of rectangular pulses 1 μsecond long spaced 1 millisecond apart. To examine them on a time base would be very difficult, but an application of Fourier analysis enables us to transform the problem to an examination of the power output on a frequency base i.e. the spectrum.

Fourier analysis of pulsed output

Our time base function describing the transmitter output (figure 3.8) may be represented as f(t).

We have therefore $f(t) = \sum_{n=-\infty}^{\infty} a_n \exp(in\omega t)$

where $a_n = \frac{\omega}{2\ell} \int_{-\ell}^{\ell} f(t) \exp(-in\omega t)\, dt$

and $f(t) = b \sin \omega_0 t \quad -\tau/2 < t < \tau/2, \quad f(t) = 0 \quad |t| > \tau/2$

Inserting the value of f(t) into the integral, we find that a_n is not significantly different from zero except for values of n in the neighbourhood of 10^4. Plotting the right hand side of equation 1 gives figure 3.9. Since n takes on integral values only this is a line spectrum, but there are 2,000 lines in the center maximum, so that n may be treated as a continuous variable.

The spectrum of the modulating waveform could be calculated analytically, but it is easier to superimpose graphically ten spectra such as figure 3.9, the center of each shifted an appropriate amount in frequency (figure 3.10). This is justified because the power

measuring device gives average power over the 0.01 second modulation period.

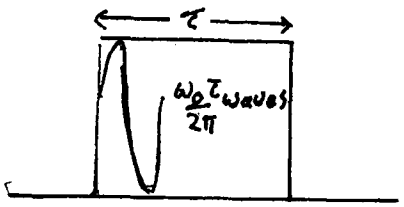

Figure 3.8
Transmitter pulse

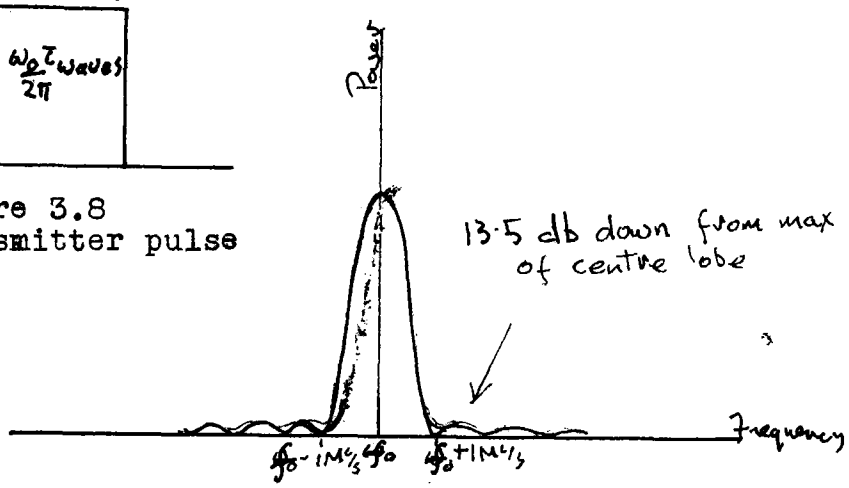

Figure 3.9 Spectrum of pulse shown in figure 3.8

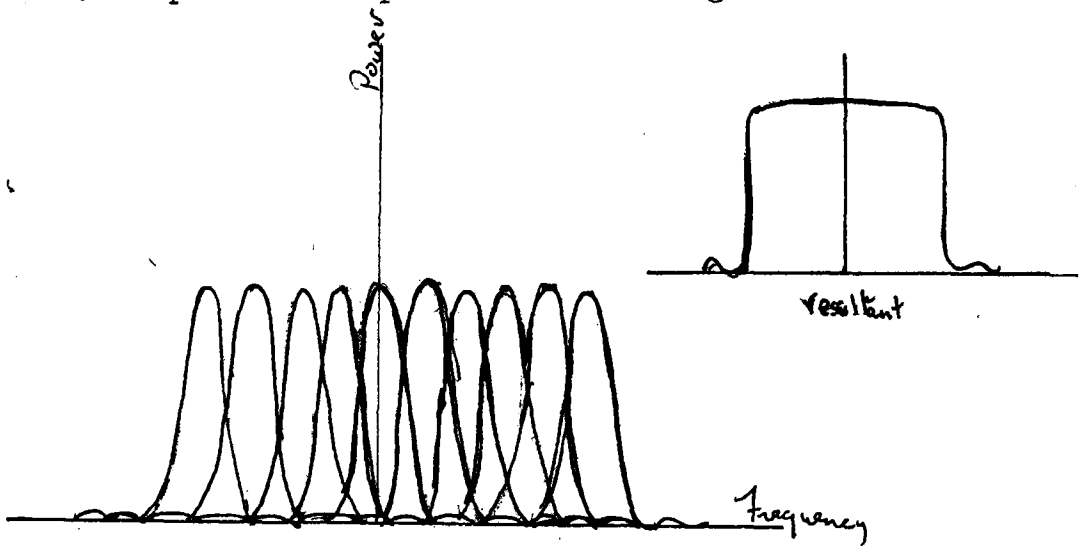

Figure 3.10 Spectrum of transmitter output with frequency modulation from pulse to pulse.

The position of the first minimum in figure 3.9 is determined by the pulse repetition frequency. For a P.R.F. of 1,000 it is $1M^c/_s$ away from f_o

Interpretation of spectrum

Departure of the spectrum from the ideal gives an indication of the behaviour of the magnetron during the pulse. Figure 3.11 adapted from Montgomery gives some typical spectra with associated pulse types.

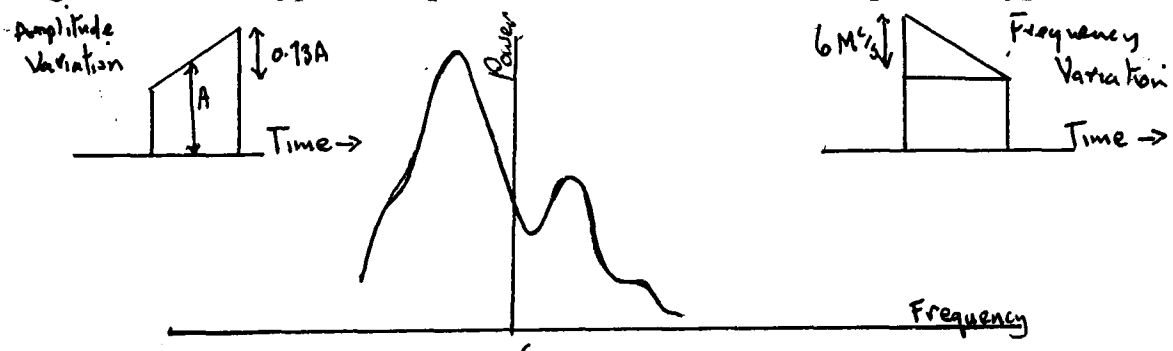

Linear frequency modulation combined with linear amplitude modulation.

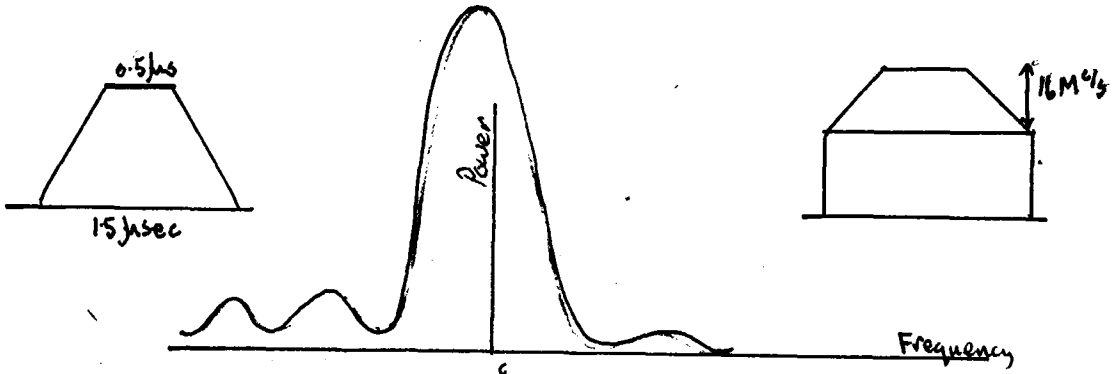

Trapezoidal pulse with frequency modulation.

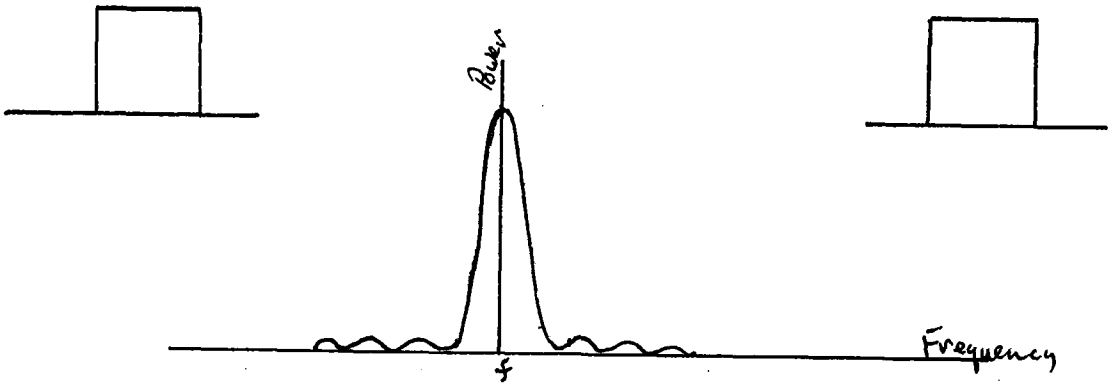

Ideal case; no amplitude or frequency modulation.

Figure 3.11 Spectra associated with some pulse types. The central frequency f is that of the r.f. wave under the pulse envelope.

Apparatus used

The spectrum analysis is carried out with an echo box and an amplifier. The echo box consists of a loosely coupled cavity resonator followed by a crystal detector. The combination was calibrated (output meter reading against db below full scale deflection) for a certain setting of amplifier gain by the use of a slotted section terminated by a short circuit.

This method utilises the properties of standing waves on a transmission line. The law governing the voltage at a point on a transmission line or waveguide is

$$\left|\frac{V_x}{V_r}\right| = \left\{\sinh^2(u+\alpha y) + \cos^2(v+\beta y)\right\}^{\frac{1}{2}}$$

where V_x is the voltage at a given point, V_r that at a reference point, y is the distance from the reference point; u and v are defined by $k_T = \exp -2(u+jv)$ k_T being the reflection coefficient at the point where the standing waves originate, and α and β the real and imaginary parts of the propagation constant $\gamma = \alpha + j\beta$. In our case, the waveguide may be assumed perfectly lossless so that $\alpha = 0$.

Our reflecting surface is assumed to be a perfect short circuit so that $k_T = 1$, $u = 0$, $\frac{V_x}{V_r} = \cos\beta y$ i.e. V_x is $\log\cos\beta y$ db below V_r.

When $V_x = V_r$, $y = 0$, so our reference point is a maximum of voltage. Finally $\beta = \frac{2\pi}{\lambda}$ where λ is the guide-

wavelength, and since βy increases by π from one minimum to the next ($V_x = 0$), the distance between minima is $\lambda/2$.

Our method involves first the measurement of the guide wavelength. This is done by locating the positions of the probe in the slotted line at which the signal is at a minimum, and measuring the distance between them.

Next a maximum is located on the slotted line, and the amplifier gain adjusted to give an output meter reading of full scale. A series of values, output meter reading against distance of the probe from the position of maximum reading, is obtained; this gives a series of y's ; they are put into the expression $\log\cos \beta y$ to give the value of attenuation below full scale deflection corresponding to the associated meter reading.

The amplifier may be assumed to be linear in response over small ranges of gain variations, so that if for a given measurement of the transmitter output it is necessary to alter the gain a little in order to make the maximum output give full scale deflection, the calibration is still valid.

The echo box resonator is tuneable, its dial is calibrated in 0.2M% steps and its bandwidth is roughly 0.2M%

This finite bandwidth is a source of serious

inaccuracy in plotting spectra. It results in a filling up of the minima in the spectrum as illustrated in figure 3.12. Here the dotted line represents the band-pass characteristic of the echo box; it is being used to "scan" the spectrum shown as a solid line.

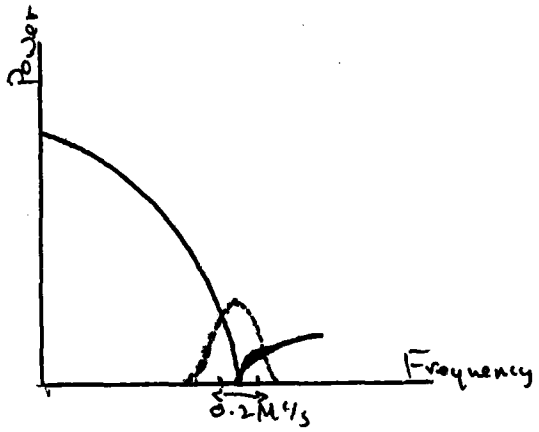

Figure 3.12 Effect of bandwidth on power output of echo box at the minima of the spectrum.

Chapter IV

RESULTS OBTAINED

When the time for the installation of the frequency modulation came, the radar was found to be operating poorly. The power output was varying erratically over a range of about 5 db, the period of the variations being of the order of 10 seconds. This made it impossible to make a satisfactory measurement of the characteristics of the polystyrene vane.

Choice of dielectric

The lucite with which the preliminary measurements were made was found unsuitable because of its comparatively high loss tangent, which caused it to heat up.

An effort was made to use a composite vane consisting of a frame of lucite filled with a mixture of paraffin wax and titanium dioxide. It was hoped that, because of the high dielectric constant of the titanium dioxide a smaller composite vane would give the same frequency swing as a larger vane made completely of lucite. This in turn would make the construction easier and would reduce the size of the slot in the waveguide. However the composite vane heated up so much that the wax softened, so it had to be abandoned.

Speed regulation

The polystyrene vane was mounted in a polystyrene

shaft, which in turn was attached by a collar to the shaft of an electric motor. The motor was a 6 volt automobile fan motor, and was driven by A.C. from a variac. This enabled the speed to be adjusted. A voltage of about 7 v. was found necessary to make the motor turn at 3,000 rpm. The speed was checked with a stroboscopic lamp. The vane appeared to be stationary at several readings of the stroboscope, so a group of readings was taken in order to determine the fundamental. Thus the vane appeared stationary at a reading of 3,000, 1500, 1000, 750 rpm, which leaves no doubt as to the actual speed, 3,000 rpm.

Transmitter spectrum

The next step is to examine the transmitter spectrum with the vane stationary. This is shown in figure 4.1.

Reference to figure 3.11 enables us to interpret this spectrum: it shows that the pulse is both frequency and amplitude modulated.

It may be noted that the mere fact that the spectrum is asymmetrical is sufficient to indicate that the pulse is modulated in amplitude and frequency, since the assymetry shows that the higher frequencies are weighted relative to the lower, or vice versa. The spectrum obtained with the echo box is not very accurate as pointed out on page 28, so an exact comparison can not be made with the sketch of figure 3.11.

Thus we can not use figure 4.1 to estimate the amount of modulation in the pulse.

Figure 4.2 shows the transmitter spectrum measured with the vane rotating, and figure 4.3 shows the composite spectrum built up by superimposing that of figure 4.1 ten times.

The construction of the composite spectrum is slightly different from the case considered in chapter III because there we assumed a sawtooth modulation, where as in the practical case we have a sinusoidal modulation. Reference to figure 3.3 enables us to see the necessary changes needed to account for this. Successive pulses have the mean frequencies f, (f+1), (f+3.5), (f+6.5), (f+9), (f+10), (f+9), (f+6.5), (f+3.5), (f+1). This gives the amount by which the individual spectrum must be

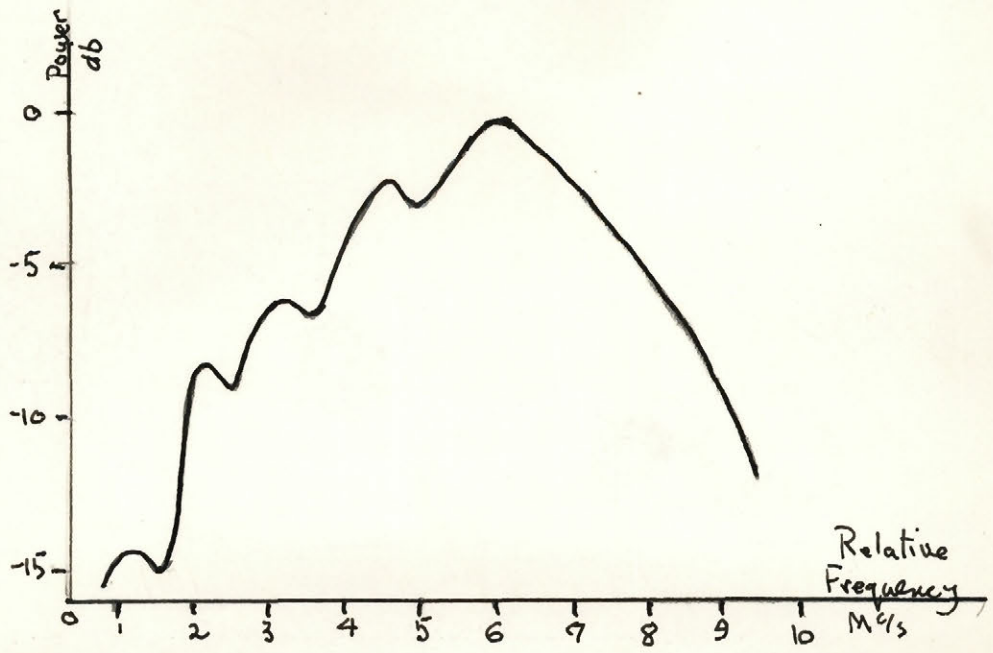

Figure 4.1 Transmitter spectrum with frequency shifting vane stationary.

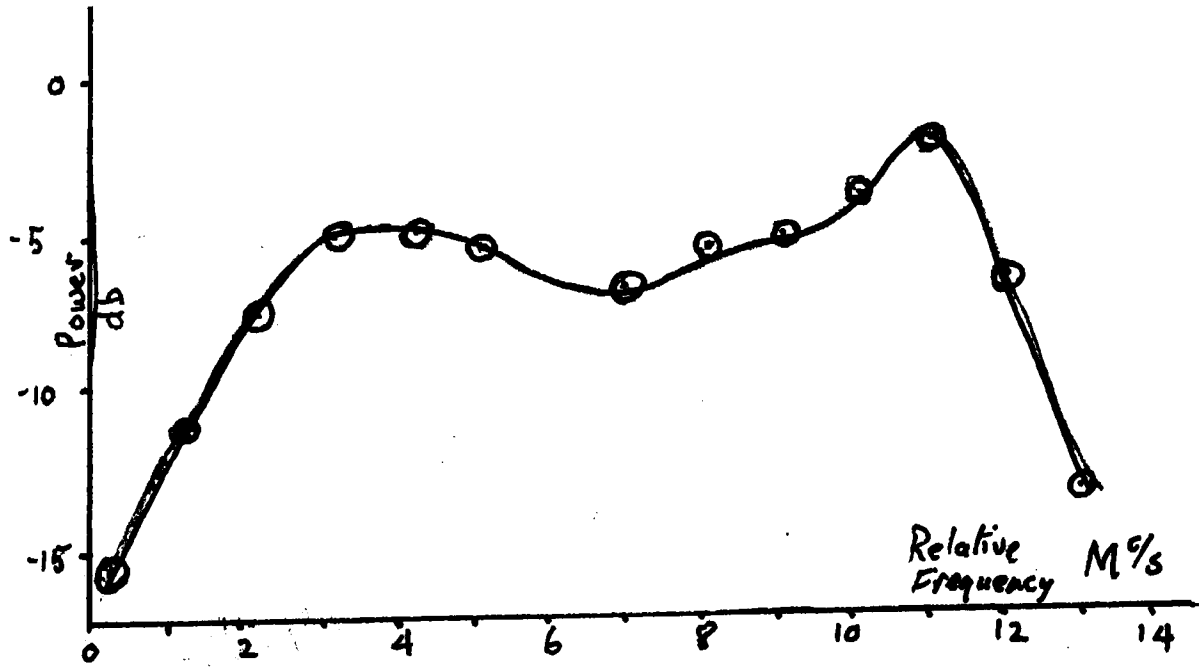

Figure 4.2 Transmitter spectrum with the frequency shifting vane rotating.

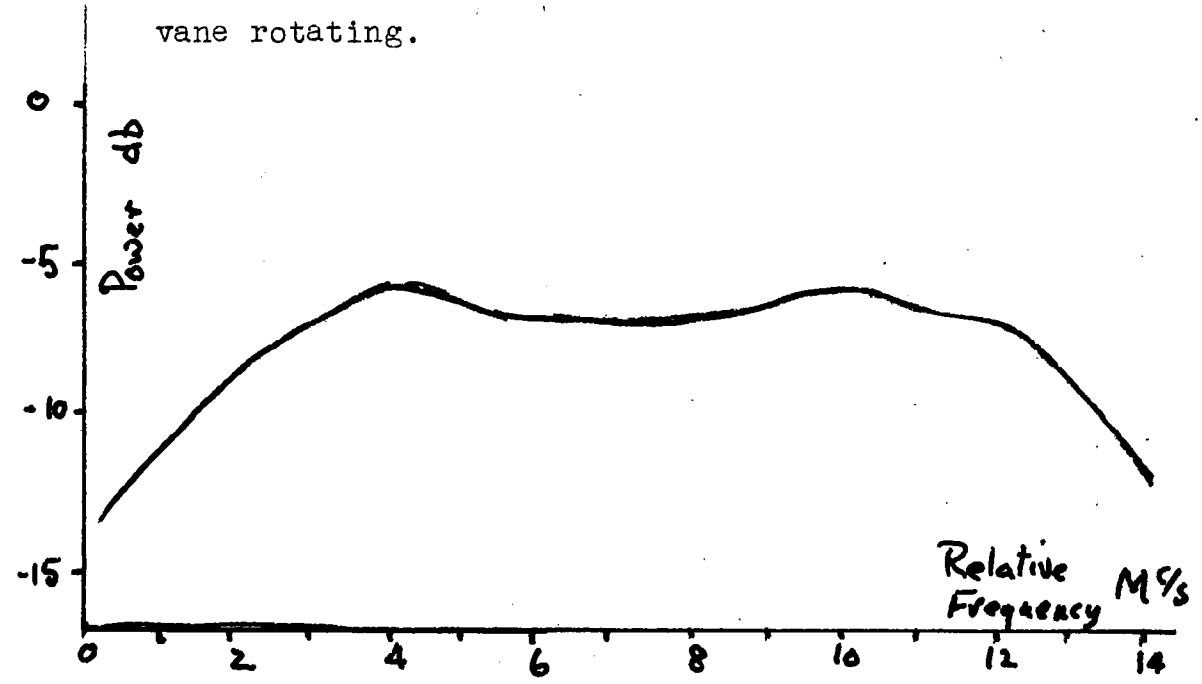

Figure 4.3 Spectrum built up by the superimposition of the spectrum of figure 4.1 ten times. Vertical scale reduced by a factor of ten.

displaced namely 1, 3.5, 6.5, 9, 10Mc/s. Moreover all the individual spectra except the first and last (0 and 10Mc/s displacement) must be given double weight, since they occur both on the rising and falling part of the sine curve.

The calculation above is based on a frequency modulation amplitude of 10Mc/s. If a shift of less than 10Mc/s, say Δf, takes place, the displacements must all be reduced by the ratio $\Delta f/10$.

In constructing the composite curve of figure 4.3 it was found in fact that the best fit to figure 4.2 was obtained on the assumption of a total frequency modulation amplitude of 8Mc/s.

Figure 4.2 leaves no doubt that the frequency of the set is being modulated. Comparison of figure 4.2 and figure 4.3 enables us to say with confidence that the modulation envelope is sinusoidal, and the amplitude 8Mc/s.

Power changes

Changes in the power output as the vane rotates may be due to two causes: movement about the Riecke diagram causes a change in the actual output of the magnetron, and secondly the absorbtion in the vane reduces the power delivered to the antenna.

The question of possible power changes from pulse to pulse can not be satisfactorily settled until the

performance of the radar is improved. The unsteadiness in the power output makes it impossible to check the power to better than about 5db. However in earlier tests made with the lucite it was found that the power did not vary by more than 2db as the vane was rotated slowly.

Use of the polystyrene vane will not change the power losses due to movement on the Riecke diagram, and the losses caused by absorption are certainly less in polystyrene than in lucite. Hence we can deduce that the power changes during the modulation cycle using a polystyrene vane are less than 2db.

Chapter V

THE MICROWAVE GYRATOR

A new device has been announced which seems to be more promising for our purpose than the rotating vane. It is the microwave gyrator (Hogan, 1952).

This device utilises the strong Faraday effect shown by some substances. This effect is the rotation of the plane of polarisation of radiation when passed through a magnetized sample of the substance, the rotation being proportional to the magnetization.

The use of the gyrator as a circuit element is illustrated in figure 5.1. The radiation passes down a rectangular guide A in the TE_{10} mode, enters a section of cylindrical guide through a transition B, and passes through the gyrator C. Its plane of polarisation is rotated, it carries on to be reflected at D back through the gyrator and its plane of polarisation is further

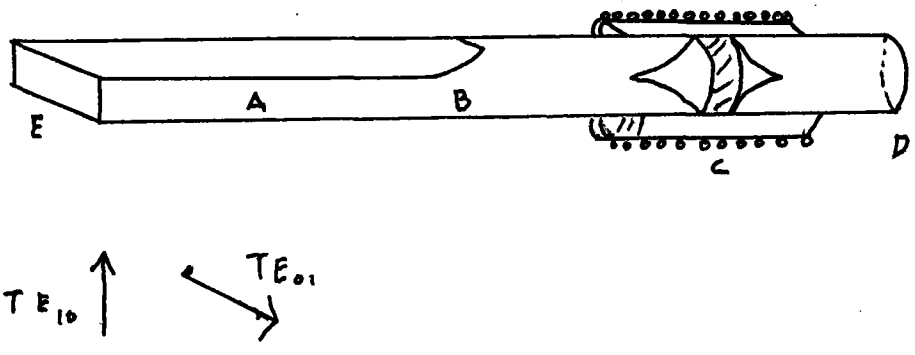

Figure 5.1 Use of a gyrator as a reactor which can be varied by v arying the magnetization.

rotated in the same direction as before. Hence on arriving back at A it has a component in the TE_{01} mode. This component is removed by a filter inside the waveguide, and so the amount of power leaving the guide at E is less than that entering.

We propose that this device may be used as a variable reflector to replace the rotating vane.

The amount converted into the TE_{01} depends on the degree of rotation undergone in the gyrator; this depends on the size of the magnetic field set up by the electromagnet. But the amount of power converted into the TE_{01} mode determines the amount in the TE_{10} mode leaving the guide at E. Thus we can vary the amount of reflected energy by varying the current in the electromagnet.

But as we have seen, the amount of reflected energy can determine the frequency of a magnetron. Hence we have a convenient way of modulating the magnetron frequency.

It has the advantage that, being purely electrical, it is more flexible than the rotating vane method. A variety of modulation envelopes could be devised for special purposes, such as eliminating ghost echoes.

The Faraday effect in Ferramic A is reported by Hogan to be 45 degrees/cm at 500 oersteds. This indicates that the fields needed could be readily obtained by an electromagnet. The rapid variation of the field might be a difficult task however.

Chapter VI

SUMMARY AND CONCLUSIONS

We have seen in the preceding chapters that frequency modulation will result in an improvement of the performance of a radar set used for observation of atmospheric precipitation, by making the echo received a more exact measure of the amount of precipitation causing the echo, than it is in the unmodulated case.

An examination of the characteristics of the magnetron oscillator has been made, possible methods of frequency modulating the magnetron have been discussed, and the conclusion reached that only one method is suitable.

This method involves periodically changing the standing wave ratio in the waveguide fed by the magnetron. A simple mechanical method has been devised to do this, namely a rotating vane introduced into the waveguide.

The construction of this apparatus has been completed and evidence obtained from spectrum analysis that the vane was in fact modulating the magnetron.

A method of varying the klystron frequency in step with the magnetron frequency has been devised and a circuit assembled to do this.

In the course of the work certain disadvantages

of the rotating vane method made themselves felt. It is difficult to get a frequency swing of the desired size with a vane large enough to fit into the waveguide, and it would be difficult to get the sawtooth waveform which is desired.

Another disadvantage is the difficulty of synchronising the klystron sweep with the magnetron sweep. This difficulty would be greatly magnified if any but the simplest modulation waveform were used.

In order to overcome these disadvantages we have proposed a method of changing the standing wave ratio in the waveguide, and hence the magnetron frequency, by a purely electrical means. This involves the use of a microwave gyrator. No experimental work has been done on this.

APPENDIX

Specification of AN/TPS 10 Radar

Type	AN/TPS 10 (United States army)
Power output (nominal)	peak average
	65Kw 65 watts
Wavelength	3.3cm
Power tube	magnetron 2J49
Pulse length	1μsec, 0.3Km, 984 feet
PRF	1000 per second
Beam width	azimuth 2^{o}
	elevation $1/2^{o}$ to 1/2 power
Scanning cycle	25^{o} in elevation in 1 second
Local oscillator	2K25 Klystron
AFC	gas control tube
Display	A type and Range Height Indication.

REFERENCES

Hogan, C. L., 1952: The Ferromagnetic Faraday Effect at Microwave Frequencies and its Application --- The Microwave Gyrator. Bell System Technical Journal, January 1952.

Marshall, J. S. and Walter Hitschfeld, 1951: Interpretation of the Fluctuating Echo from Randomly Distributed Scatterers. Research Report MW-4, Stormy Weather Research Group, McGill University.

Montgomery, Carol G. (editor): Technique of Microwave Measurements. Radiation Laboratory Series, Volume 11, McGraw Hill, 1950.

R.L. Series, Volume 6: Microwave Magnetrons. George B. Collins (editor). Radiation Laboratory Series, Volume 6, McGraw Hill, 1950.

Slater, John C.: Microwave Electronics. Van Nostrand, 1950.